*Egypt. J. Chem.* **Vol. 68**, No. 12 pp. 1 - 10 (2025)

**Egyptian Journal of Chemistry**

**http://ejchem.journals.ekb.eg/**

# Cellulose Nanofibers for Efficient Adsorption of Hexavalent Chromium Ions

**Hanan Awydat [a], Fatma T. Abdelwahed [a], Naglaa Salem El-Sayed [b*], Mohamed M. El Defrawy [a], Rania M. Eltabey [a*]**

[a] *Chemistry Department, Faculty of Science, Mansoura University, Mansoura, Egypt*
[b] *Cellulose and Paper Department, National Research Centre, 33 El Bohouth St., Dokki, P.O. 12622, Giza, Egypt*

**Abstract**

A TEMPO-oxidized cellulose nanofiber (CNF) was synthesized and characterized using FTIR, XRD, and TEM to confirm its structural and functional properties. This modified CNF was then applied as an adsorbent for removing Cr(VI) from aqueous solutions. Key parameters affecting the adsorption process, including pH, sorbent dosage, initial Cr(VI) concentration, contact time, temperature, as well as desorption conditions, were systematically studied. The results revealed that the CNF exhibited an impressive adsorption capacity of 302.0 mg $g^{-1}$ for Cr(VI) at optimum conditions of pH 2.0, 0.03g (dose), 60 min, and 25 $^{o}$C. Moreover, kinetic studies indicated that the process fitted well with pseudo-second-order kinetics, while equilibrium data were best described by the Freundlich isotherm, suggesting a heterogeneous, multi-layer adsorption mechanism. Furthermore, the obtained results revealed that 90% of adsorbed Cr(VI) could be regenerated by using 0.1 M NaOH even after three adsorption-desorption cycles.

**Keywords**: Cr(VI) removal, CNF, Freundlich isotherm, adsorption kinetics, adsorption capacity

## 1. Introduction

The valorization of biomass waste involves converting organic residues, such as agricultural by-products, food waste, and industrial organic residues, into commercially valuable products. This process leverages chemical, thermal, biological, or electrochemical methodologies to transform what would otherwise be an environmental burden into renewable energy sources, biochemicals, or high-performance materials. By implementing integrated biorefinery approaches, multiple products with added value can be produced from a single biomass source. For example, biomass can be processed through thermochemical methods like pyrolysis or gasification to yield biofuels and biochar, or through biochemical routes such as anaerobic digestion and fermentation to produce biogas and bioethanol [1]–[3]. These cascaded processing strategies maximize resource efficiency, minimize waste, and contribute significantly to the principles of a circular economy [3], [4]. Valorization not only reduces waste disposal challenges and environmental pollution but also fosters economic growth by opening new revenue streams. Additionally, it contributes to a reduction in greenhouse gas emissions and decreases reliance on fossil fuels, aligning with global sustainability and climate goals [5], [6].

Chromium (Cr(VI)) is commonly used in electroplating, leather tanneries, and metal finishing processes [7]. Cr(VI) is one of the most hazardous chemicals that has carcinogenic and toxic effects on human health, including nausea, vomiting, dermatitis, and liver and kidney damage [8]. Various methods, including flocculation, cloud point extraction, liquid-liquid extraction, photocatalysis, and adsorption, have been reported for treating polluted water [9]–[16]. Amongst them, adsorption is widely used owing to its simplicity, effectiveness, affordability, and high removal efficiency. Cellulose, a widely abundant polysaccharide, has a long chain of β-D-glucopyranose units connected to form an unbranched homopolysaccharide by β (1→4) glycosidic bonds [17]. Due to its numerous hydroxyl groups, cellulose interacts effectively with water pollutants. Since natural cellulose is less stable and has poor adsorption capabilities, many studies have tried to modify cellulose to enhance its adsorption performance [18]. Cellulose nanofiber (CNF) comprises unique characteristics, including lightweight, strong, biodegradable, and renewable, making them highly appealing in diverse applications such as water treatment, packaging, biomedical fields, and electronics [19]. *Bettaieb et al.* prepared a composite of CNF and polyethylenimine for methyl orange dye removal, reaching a maximum adsorption capacity of 313 mg $g^{-1}$ [20]. In another study, *Shao et al.* functionalized CNF with polypyrrole, generating a composite that was active in the removal of Cr(VI) [21].

In this work, cellulose nanofiber extracted from the bleatched pulp of sugarcane bagasse was modified via the TEMPO-oxidization to introduce carboxyl functionality and increase its adsorption capacity. The prepared nanocomposite was characterized using FTIR, XRD, and TEM. CNF was applied for Cr(VI) adsorption from aqueous solutions. The variables influencing adsorption capacity were studied, including pH, dose, time, concentration, and temperature. Reusability studies of TEMPO-Oxidized CNF were performed for three adsorption-desorption cycles with a removal efficiency of 90 %. This work

*Corresponding author e-mail: ns.salem@nrc.sci.eg (Naglaa Salem EL-Sayed)& reltabey@mans.edu.eg(Rania M. Eltabey).

Received date 01 June 2025; Revised date 29 June 2025; Accepted date 20 July 2025
DOI: 10.21608/ejchem.2025.390208.11842

makes the development of an environmentally friendly and highly effective adsorbent for the Cr(VI) adsorption from wastewater possible.

## 2. Results and discussion

### 2.1. Characterization of cellulose nanofibers

#### 2.1.1. Fourier-transform infrared (FTIR)

The FTIR spectra of CNF and TEMPO-oxidized CNF were shown in Fig. 1; the cellulose characteristic peaks, including stretching vibrations of –OH and inter/intramolecular hydrogen bonds (3336 $cm^{-1}$), $–CH_2$ (2895 $cm^{-1}$), and C–O–C (1031 $cm^{-1}$) were observed [13]. After TEMPO-oxidization, the band at 1732 $cm^{-1}$ was appeared ascribed to the asymmetric vibration band of carboxylic carbonyl suggesting successful oxidation of CNF [23]. Furthermore, shifts of OH band after TEMPO-oxidized was observed from 3336 to 3312 $cm^{-1}$ and $–CH_2$ stretching vibrations to 2853 $cm^{-1}$.

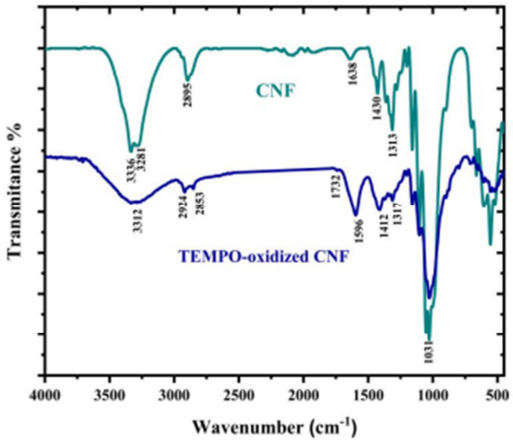


**Figure 1:** FTIR spectrum of CNF and TEMPO-oxidized CNF

#### 2.1.2. X-ray diffraction (XRD)

Fig. 2 shows the XRD diffractogram for TEMPO-oxidized CNF. hree characteristic peaks of the native cellulose I polymorph are clearly observed at 2θ = 18.05° (broad, (110) plane), 22.37° (sharp and intense, (200) plane) and 34.16° (small, sharp, (004) plane), confirming that TEMPO oxidation preserves the underlying crystalline framework of CNF [24]. According to Segal Crystallinity Index (CrI) equation [1]

$$CrI\ (\%) = [(I200 – Iam) / I200] \times 100 \quad [1]$$

The calculated CrI was found to be 85.2%, the Scherrer analysis of the (200) reflection yields a crystallite size of 81 nm and a microstrain of 0.00218 (0.218 %). These data strongly suggest that the TEMPO oxidation for bagasse pulp preserves the cellulose I crystalline framework with only minimal lattice distortion [5, 22].

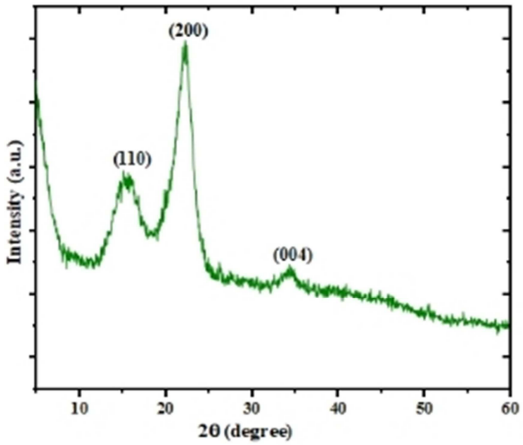


**Figure 2:** XRD spectrum of TEMPO-oxidized CNF

2.1.3. TEM

The TEM image of TEMPO-oxidized CNF revealed in Fig. 3, displayed a sparsely distributed nanofiber or nanotube-like structure on a light gray background, providing a good synthesis of CNF.

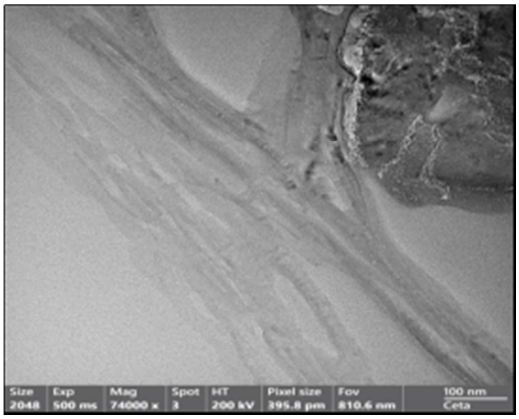


**Figure 3:** TEM image of TEMPO-oxidized CNF.

2.2. Adsorption studies

2.2.1. Influence of pH

pH is a crucial parameter during the Cr(VI) adsorption process; the adsorption capacity reaches its maximum value at pH 2.0 (Fig. 4). Whereas, with the increase of pH, the TEMPO-oxidized CNF adsorption capacity gradually decreases until it reaches lower values in the basic medium. This change can be attributed to the dominant species of chromium at pH (2.0-6.0) present as $HCrO_4^-$ and $Cr_2O_7^{2-}$ and hence, attraction forces with positively charged hydroxyl and carboxylic groups occur [25]. In the basic medium, on the modified CNF surface, the $OH^-$ and chromium anions will compete for the adsorption sites.

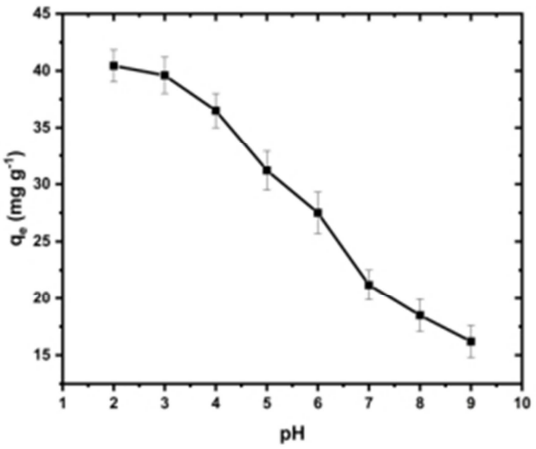


**Figure 4:** Effect of pH on adsorption of Cr(VI) by TEMPO-oxidized CNF.

2.2.2. Influence of dose

The effect of TEMPO-oxidized CNF dosage for the effective Cr(VI) adsorption was performed within the range of (0.005-0.040) g. As revealed in Fig. 5, the adsorption capacity was significantly increased with the adsorbent dosage increasing until it reached equilibrium at 0.03 g owing to the abundant adsorption sites. The saturation of the TEMPO-oxidized CNF adsorption sites may be the cause of the negligible change in adsorption capacity with additional adsorbent dosage (beyond 0.03 g) [26]. Hence, 0.03 g was used for further experiments.

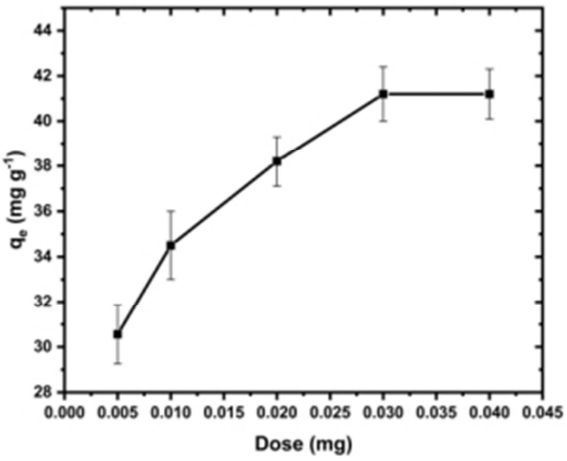


**Figure 5:** Influence of dose on adsorption of Cr(VI) by TEMPO-oxidized CNF.

2.2.3. Influence of contact time and kinetics

The effect of equilibrium time on Cr(VI) adsorption capacity at $C_i$=50 mg $L^{-1}$ was investigated (Fig. 6). The adsorption capacity increased instantly within the first 30 min and then gradually became slow due to the saturation of TEMPO-oxidized CNF adsorption sites until equilibrium was attained at 60 min [27]. The pseudo-first-order (PFO) and pseudo-second-order (PSO) kinetic models in their non-linear form were utilized to explain the kinetic adsorption process and their relative equations are shown below [28]:

Pseudo-first-order $q_t = q_e (1 - e^{-K_1 t})$ (3)

Pseudo-second-order $q_t = \frac{K_2 qe^2 t}{1 + K_2 qe\, t}$ (4)

Where $q_e$ and $q_t$ symbolize the quantity of Cr(VI) adsorbed on TEMPO-oxidized CNF at equilibrium and at a given time, respectively, $k_1$ and $k_2$ refer to the rate constants. The Cr(VI) adsorption kinetic models were displayed in Fig. 6, and their relative parameters were revealed in Table 1. By comparing the correlation coefficients ($R^2$), the PSO was assigned to be a better kinetic model for explaining Cr(VI) adsorption kinetics, which indicated that Cr(VI) adsorption onto TEMPO-oxidized CNF was mediated by chemical adsorption [29].

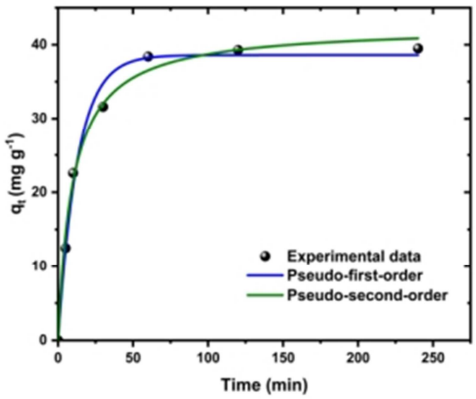


**Figure 6:** Effect of time and kinetic fittings of Cr(VI) adsorbed onto TEMPO-oxidized CNF.

**Table 1:** Kinetic parameters for Cr(VI) adsorbed by TEMPO-oxidized CNF.

| Models | adsorbent@Cr(VI) |
|---|---|
| Pseudo 1st order | |
| $q_e$ (exp)(mg $g^{-1}$) | 40.56 |
| $q_e$ (cal)(mg $g^{-1}$) | 38.60 |
| $K_1$($min^{-1}$) | 0.077 |
| $R^2$ | 0.989 |
| Pseudo 2nd order | |
| $q_e$ (exp)(mg $g^{-1}$) | 40.56 |
| $q_e$ (cal)(mg $g^{-1}$) | 42.53 |
| $k_2$ (g $mg^{-1}$ $min^{-1}$) | 0.002 |
| $R^2$ | 0.992 |

2.2.4. Influence of concentration and isotherm studies

The equilibrium adsorption isotherm is essential for examining the behavior of interactions between the adsorbent and Cr(VI). The non-linear Langmuir and the Freundlich adsorption isotherm models simulated the equilibrium adsorption data. Their respective non-linear equations are shown below [30], [31]. The non-linear curves and parameters are depicted in Fig. 7 and Table 2, respectively. By comprehensively comparing the two isotherm models, the adsorption data was more accurately described by the Freundlich model, according to the ($R^2$) value [32]. The calculated n value (Table 2) is higher than 1.0, suggesting favorable and feasible adsorption of Cr(VI) on TEMPO-oxidized CNF.

Langmuir equation $q_e = \frac{Q_{max} K_L C_e}{(1+K_L C_e)}$ (5)

Freundlich equation $q_e = K_F C_e^{1/n}$ (6)

where $Q_{max}$ is the maximum adsorption amount; $K_L$ and $K_F$ are the Langmuir and Freundlich isotherm constants, respectively. n stands for the adsorption intensity.

**Table 2:** Isotherm parameters for Cr(VI) adsorbed by TEMPO-oxidized CNF.

| Models | adsorbent@Cr(VI) |
|---|---|
| Langmuir | |
| $Q_{max}$ (mg $g^{-1}$) | 418.7 |
| $K_L$ (L $mg^{-1}$) | 0.035 |
| $R^2$ | 0.857 |
| Freundlich | |
| $K_f$ | 52.82 |
| n | 2.495 |
| $R^2$ | 0.966 |

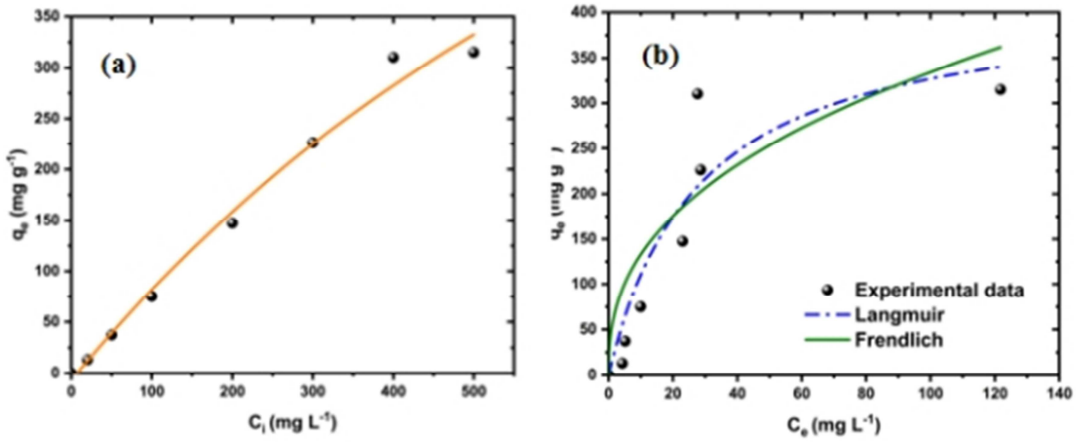


**Figure 7:** Effect of concentration and isotherm fittings of Cr(VI) adsorbed onto TEMPO-$_{\text{oxidized CNF}}$.

2.2.5. Thermodynamic studies

Using van't Hoff equation, the impact of temperature in the 298–318 K range was investigated to explain the Cr(VI) thermodynamic process. The thermodynamic equations used were [33]:

$$\mathbf{\Delta G = -RT \ln} K_L \quad (7)$$

$$\boldsymbol{\Delta G = \Delta H - T\Delta S} \quad (8)$$

ΔG (kJ mol−1) is the Gibbs energy change, ΔH is the enthalpy change (kJ mol−1), and ΔS (kJ·mol$^{-1}$·K$^{-1}$) denotes the entropy change. Here, R is the universal gas constant (8.314 × 10$^{-3}$ kJ·mol$^{-1}$·K$^{-1}$), and T is the absolute temperature in kelvin (K). KL is constant calculated from dividing Qe and Ce. ΔH and ΔS were attained from the slope and intercept of the plot of ln KL versus 1/T. The equilibrium adsorption of Cr(VI) was elucidated by fitting the 1/T versus lnKL. The thermodynamic parameters are shown in Fig. 8 and Table 3. The *ΔG* negative values revealed the spontaneity of the adsorption. Furthermore, the endothermic and random nature of the Cr(VI) adsorbed by TEMPO-oxidized CNF was indicated by the positive values of Δ*H*0 and Δ*S*0 [34].

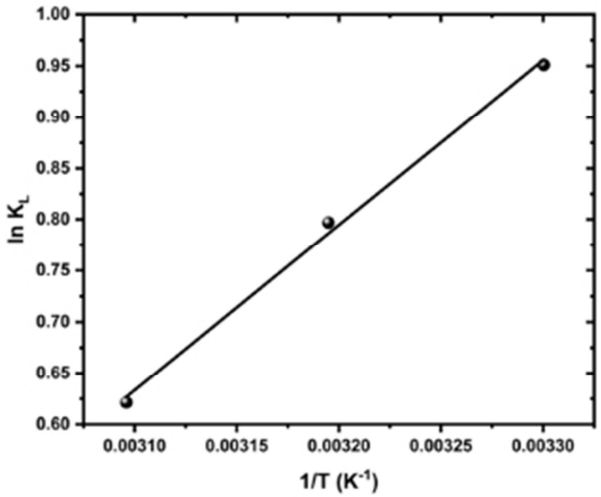


**Figure 8:** Plot of reciprocal of temperature (1/T) versus ln $K_L$ of Cr(VI) adsorbed onto TEMPO-oxidized CNF.

**Table 3:** Thermodynamic parameters for Cr(VI) adsorbed by TEMPO-oxidized CNF.
$pH_0$ = 2.0, agitation time = 60 min, adsorbent dose = 0.03g.

| Sample | $\Delta H^\circ$ (kJ $mol^{-1}$) | $\Delta S^\circ$ (J $mol^{-1}$ $K^{-1}$) | $-\Delta G^o$ (kJ $mol^{-1}$) | | |
|---|---|---|---|---|---|
| | | | 303k | 313k | 323k |
| TEMPO-oxidized CNF | 13.39 | 36.26 | 2.39 | 2.07 | 1.67 |

2.2.6. Desorption and reusability studies

To evaluate the reusability of TEMPO-oxidized CNF adsorbent, 3 adsorption–desorption cycles were conducted. The Cr(VI) was regenerated by dipping it into NaOH solution (0.1 mol L-1, 20 ml) and stirring for 20 min. After 3 cycles, the removal efficiency exceeded 90% as more Cr(VI) can be captured by the adsorbent after NaOH treatment. Under acidic conditions, the majority of Cr(VI) ions were adsorbed as negatively charged species such as $HCrO_4^-$ or $Cr_2O_7^{2-}$ through electrostatic attraction. Raising the pH, using NaOH solution as a desporing agent, causes the adsorbent surface to become negatively charged, which repels and desorbs Cr(VI) ions back into solution. Providing high stability as well as good separation of the prepared adsorbent [35], as shown in Fig. 9.

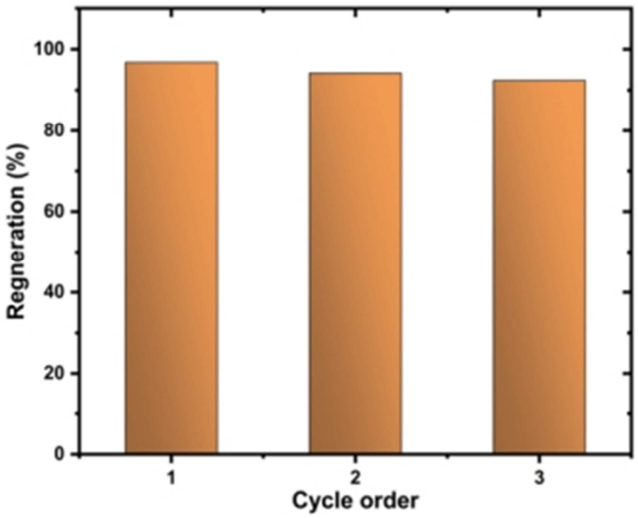


**Figure 9:** Desorption study with NaOH (0.1 mol $L^{-1}$).

2.2.7. Comparison with different adsorbents

Table 4 compares the adsorption capacity and optimum conditions for Cr(VI) adsorption onto TEMPO-oxidized CNF with other adsorbents. The data imply the ability of TEMPO-oxidized CNF to adsorb Cr(VI) effectively with high adsorption capacity. According to the data obtained from pH effect, the TEMPO-oxidized CNF showed higher adsorption capacity values in acidic medium compared to that in basic medium which suggests that the electrostatic attraction between Cr(VI) and positively charged hydroxyl and carboxylic groups strongly affect the adsorption capacity. Also, hydrogen bondings could be performed. Therefore, the mechanism of interaction between Cr(VI) and TEMPO-oxidized CNF could be summarized as evaluated in Fig. 10.

**Table 4:** Comparing Cr(VI)'s adsorption capabilities onto TEMPO-oxidized CNF with those of other adsorbents.

| Adsorbent | Conditions | Qe (mg $g^{-1}$) | Ref |
|---|---|---|---|
| nanofibrillated cellulose/chitosan aerogel | pH=3.0, t=120min | 197.3 | [36] |
| Cellulose@PEI aerogel | pH=2.0, m=0.02g | 229.1 | [37] |
| Amino-functionalized magnetic cellulose | pH=3.0, t=120min, m=0.02g | 171.5 | [38] |
| $Fe_3O_4$-coated CA/CS nanofibers | pH=3.0, t=120min, m=0.4g | 193.2 | [39] |
| TEMPO-oxidized CNF | pH=2.0, m=0.03g, t=60 min | 302.0 | This study |

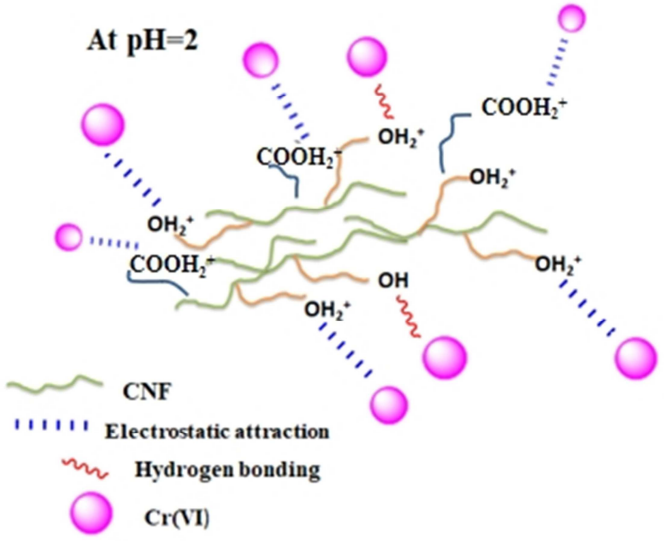


**Figure 10:** Mechanism of interactions between Cr(VI) and TEMPO-oxidized CNF.

## 3. Materials and methods

### 3.1. Materials

The bleached bagasse pulp was purchased from Qena Company of Paper Industry, Egypt, with the chemical composition of cellulose content (96%), lignin (0.92%), hemicellulose (3%), and ash content (0.85%). Chemicals, including 2,2,6,6-Tetramethylpiperidine-1-oxyl (TEMPO), 1,5-diphenyl carbazide, K2Cr2O7, HCl, and NaOH, were supplied from Alfa-Aesar.

### 3.2. Characterization

Fourier-transform infrared (FTIR) spectrum was recorded on (Nicolet 670, Thermo Nicolet, and U.S.A). X-ray diffraction (XRD, Philips PW 1800) was recorded using Cu kα radiation (40 kV and 40 mA). The TEMPO-oxidized cellulose nanofiber morphology was monitored by transmission electron microscope (TEM) (JEM-2100HR, JEOL, Japan).

### 3.3. Synthesis of TEMPO-Oxidized Cellulose Nanofiber

CNF was synthesized as stated by El-Sayed et al. [5], [22]. Briefly, the bleached sugarcane bagasse pulp (20 g) was treated with 40 % NaOH for 2 hours with mechanical stirring at 70 oC. The fibers were collected by vacuum filtration and washed with 100 mL of distilled water three times. Then, TEMPO (1.0 g) and sodium bromide (8.0 g) were finely ground in a porcelain mortar and added to water-dispersed CNFs. This was followed by adding 300 mL of (15 %) NaOCl with mechanical consistent stirring. The pH was regulated to reach a value of 10.0 until the completion of the reaction by drops of 40% NaOH solution (3 mol L-1). At the end of the reaction, the pH was neutralized to pH 7.0, and the product was washed several times with distilled water and centrifuged at 8,000 rpm. Finally, the resulting TEMPO-oxidized CNFs (CNF) were subjected to

mechanical homogenization at 10,000 rpm at 2% fiber concentration and purified by dialysis for 96h against deionized water. CNF hydrogel was kept in the refrigerator at -4 $^{o}$C until used.

### 3.4. Sorption studies

The Cr(VI) stock solution (1000 mg L-1) was made by dissolving K2Cr2O7 in distilled water and diluting this solution for subsequent adsorption experiments. Batch adsorption studies were performed, such as pH, contact time, dose, initial Cr(VI) concentration, temperature, and reusability. Typically, 0.03 g of modified CNF adsorbent was shaken (120 rpm) with 25.0 mL of Cr(VI) concentration (20-500 mg L-1) at pH (2.0-9.0) adjusted using 0.1mol L-1 HCl /NaOH, contact time of (5-240 min), dose (0.005-0.040 g) and incubation temperature (298-320K). The residual Cr(VI) concentration was determined by the diphenylcarbazide colorimetric method with a UV–vis spectrophotometer (Jasco UV-model V-530, Japan) at 540 nm. The Cr(VI) adsorption capacity (Qe) and at t time (qt) were estimated as follows:

$$qe = (Co - Ce) \times V / m \quad (1)$$

$$qt = (Co - Ct) \times V / m \quad (2)$$

C0, Ce, and Ct (mg L−1) are the initial, equilibrium, and Cr(VI) concentrations at time *t*, respectively, V (L) is the experimental solution volume, and m is the modified CNF mass.

## 4. Conclusion

A TEMPO-oxidized cellulose nanofiber was prepared and characterized by FTIR, XRD, and TEM. The prepared adsorbent was utilized for adsorbing Cr(VI) from the aqueous solutions. The factors that affected the adsorption capacity were examined, including pH, dose, time, concentration, temperature, and desorption. According to the adsorption tests, TEMPO-oxidized CNF has an adsorption capacity of 302.0 mg g-1 for Cr(VI). The adsorption kinetics, isotherms, and thermodynamics were studied to understand the mechanism of adsorption. The adsorption process fit well with pseudo-second order kinetics according to kinetic studies. Morever, the equilibrium data was best described by Freundlich isotherm, pointing to a heterogeneous, and multi-layer adsorption mechanism. According to the results of the adsorption-desorption tests, TEMPO-oxidized CNF can be considered as a promising adsorbent for the removal of Cr(VI) from wastewater.

## 5. Conflicts of interest

The authors declare there are no conflicts to declare.

## 6. References

[1] A. R. Salem, W. A. Kassab, A. M. Adel, M. El-Sakhawy, M. T. Al-Shemy, Insight into the efficient removal of Cu (II) from aqueous solutions on a biochar-alginate composite, Process Saf. Environ. Prot., 197 (2025) 106985.

[2] M. S. Hasanin, M. T. Al-Shemy, W. H. Eisa, S. Kamel, Green biodegradable ultraviolet shielding membrane-based cellulose and lignin-doped photoactive core-shell nano bimetallic, J. Environ. Chem. Eng., 13 (2025) 115176 .

[3] N. S. El-Sayed, E. Tolba, A. Salama, Valorization of Sugarcane Bagasse into Cellulose Nanofiber Containing Phosphate Groups: A New Scaffold for in Vitro Calcium Phosphate Mineralization, Chem. Africa, 2025.

[4] M. T. Al-Shemy, F. Gamoń, A. Al-Sayed, M. S. Hellal, A. Ziembińska-Buczyńska, G. K. Hassan, Silver nanoparticles incorporated with superior silica nanoparticles-based rice straw to maximize biogas production from anaerobic digestion of landfill leachate, J. Environ. Manage., 365(2024) 121715 .

[5] N. S. El-Sayed, A. Salama, V. Guarino, Coupling of 3-Aminopropyl Sulfonic Acid to Cellulose Nanofibers for Efficient Removal of Cationic Dyes, Materials, 15(2022)19.

[6] N. S. El-Sayed, T. Y. A. Fahmy, S. Kamel, Stimuli-responsive hydrogels derived from agricultural residues: an overview, Chem. Pap., (2025) 0123456789.

[7] Y. Li, T. Huang, X. Liu, Z. Chen, H. Yang, X. Wang, Sorption-catalytic reduction/extraction of hexavalent Cr(VI) and U(VI) by porous frameworks materials, Sep. Purif. Technol. 314 (2023) 123615.

[8] H. M.Perera, A. U. Rajapaksha, S. Liyanage, A.Ekanayake, R.Selvasembian, A.Daverey, M. Vithanage, Enhanced adsorptive removal of hexavalent chromium in aqueous media using chitosan-modified biochar: Synthesis, sorption mechanism, and reusability, Environ. Res. 231(2023) 115982 .

[9] M. Saeed, M. Muneer, A. ul Haq, N. Akram, Photocatalysis: an effective tool for photodegradation of dyes—a review, Environ. Sci. Pollut. Res., 29(2022)293–311.

[10] F. T. Abdelwahed, W. I. Mortada, M. M. El-Defrawy, and R. M. Eltabey, Lead extraction from food samples by combined cloud point-micro solid phase extraction, J. Food Compos. Anal., 129 (2024) 106119.

[11] F. T. Abdelwahed, R. M. Eltabey, M. M. El-Defrawy, W. I. Mortada, Dispersive liquid– liquid microextraction based on solidification of floating organic droplet and spectrophotometric determination of Allura red using green deep eutectic solvent as disperser solvent: Green profile assessment, Microchem. J., 206 (2024) 111432.

12] C. Liu, N. Fiol, J. Poch, a I. Villaescusa, A new technology for the treatment of chromium electroplating wastewater based on biosorption, J. Water Process Eng., 11(2016)143–151.

[13] R. M. Eltabey, F. T. Abdelwahed, M. M. Eldefrawy, M. M. Elnagar, Fabrication of poly ( maleic acid ) -grafted cross-linked chitosan / montmorillonite nanospheres for ultra-high adsorption of anionic acid yellow-17 and cationic brilliant green dyes in single and binary systems, J. Hazard. Mater., 439(2022) 129589.

[14] F. T. Abdelwahed, W. I. Mortada, and R. M. Eltabey, A new surfactant-based hydrophobic deep eutectic solvent for microextraction and spectrophotometric determination of Rhodamine B and Allura red in real samples, Microchem. J., 215(2025) 114273.

[15] R. E. Khalifa, M. S. Mansour, E. E. Ebrahim, I. Ashour, M. S. Elgeundi, Application of nano adsorbent of PCMC in water treatment: removal of cationic dyes, Egypt. J. Chem., 66 (2023) 697–709.
[16] S. W. Hgag, S. M. Abdel Moniem, M. E. M. Ali, M. K. Zahran, A. Barhoum, H. S. Ibrahim, Isotherm Models for Metal Removal Using Modified Graphene, Egypt. J. Chem., 67(2024) 245–252.
[17] A. El Mahdaoui, S. Radi, A. Elidrissi, M. A. F. Faustino, M. G. P. M. S. Neves, N. M. M. Moura, Progress in the modification of cellulose-based adsorbents for the removal of toxic heavy metal ions, J. Environ. Chem. Eng. 12(2024) 113870.
[18] W. I. Mortada, I. M. M. Kenawy, Y. G. Abou El-Reash, A. A. Mousa, Microwave assisted modification of cellulose by gallic acid and its application for removal of aluminium from real samples, Int. J. Biol. Macromol., 101(2017) 490–501. [19] N. R N. Rong, C. Chen, K. Ouyang, K. Zhang, X. Wang, Z. Xu, Adsorption characteristics of directional cellulose nanofiber/chitosan/montmorillonite aerogel as adsorbent for wastewater treatment, Sep. Purif. Technol., 274 (2021) 119120.
[20] F. Bettaieb, M. A. Abdelaziz, I. S. Alatawi, M. A.Aljowni, H. Parveen, S. Mukhtar, N.Omer, R. Jame, S. A. Alshareef, M. E. Owda, Y. A. Bin Jardan, Polyethylenimine-grafted cellulose nanofibril composites: Adsorbents for anionic dye removal with thermodynamic insights, Int. J. Biol. Macromol., 310 (2025)143354.
[21] Y. Shao, Z. Fan, M. Zhong, W. Xu, C. He, Z. Zhang, Polypyrrole/bacterial cellulose nanofiber composites for hexavalent chromium removal, Cellulose, 28(2021) 2229–2240.
[22] N. S. EL-Sayed, S. Dacrory, M. El-Sakhawy, E. B. Hassan, S. Kamel, Fabrication of nanocomposite based on oxidized biochar and oxidized cellulose nanofibers and its potential Cd(II) adsorption, Adsorption, 31 (2025).
[23] M. A. Hashem, M. M. Elnagar, I. M. Kenawy, M. A. Ismail, Synthesis and application of hydrazono-imidazoline modified cellulose for selective separation of precious metals from geological samples, Carbohydr. Polym., 237 (2020)116177.
[24] J. Ponce, J.G. da Silva Andrade , L.N. dos Santos, M. K. Bulla, B. C. B. Barros, S.L.Favaro, N.Hioka, W. Caetano, V. R. Batistela., Alkali pretreated sugarcane bagasse, rice husk and corn husk wastes as lignocellulosic biosorbents for dyes, Carbohydr. Polym. Technol. Appl., 2(2021) 100061.
[25] D. Chen, W. Li, Y. Wu, Q. Zhu, Z. Lu, G. Du, Preparation and characterization of chitosan / montmorillonite magnetic microspheres and its application for the removal of Cr ( VI ), 221(2013)8–15.
[26] T. C. Egbosiuba, A. S. Abdulkareem, A. S. Kovo, E. A. Afolabi, J. O. Tijani, M.T.Bankole, S. Bo, W. D. Roos, Adsorption of Cr(VI), Ni(II), Fe(II) and Cd(II) ions by KIAgNPs decorated MWCNTs in a batch and fixed bed process, Sci. Rep., 11(2021) 1–20.
[27] J. Liu, B. Zhou, H. Zhang, J. Ma, B. Mu, W. Zhang, A novel Biochar modified by Chitosan-Fe/S for tetracycline adsorption and studies on site energy distribution, Bioresour. Technol., 294 (2019) 122152
[28] A. M. Tawfik, R. M. Eltabey, Fractional Kinetic Strategy toward the Adsorption of Organic Dyes: Finding a Way Out of the Dilemma Relating to Pseudo-First- and Pseudo-Second-Order Rate Laws, J. Phys. Chem. A, 128(2024)1063–1073.
[29] W. Yao, T. Ni, S. Chen, H. Li, Y. Lu, Graphene/Fe3O4 at polypyrrole nanocomposites as a synergistic adsorbent for Cr(VI) ion removal, Compos. Sci. Technol., 99 (2014) 15–22.
[30] M. H. Armbruster, J. B. Austin, The Adsorption of Gases on Plane Surfaces of Mica, J. Am. Chem. Soc., 60 (1938) 467–475.
[31] H. Freundlich, Über die Adsorption in Lösungen, *Zeitschrift für Phys. Chemie*, 57U (1907) 385–470.
[32] C. Niu, N. Zhang, C. Hu, C. Zhang, H. Zhang, Y. Xing, Preparation of a novel citric acid-crosslinked Zn-MOF/chitosan composite and application in adsorption of chromium(VI) and methyl orange from aqueous solution, Carbohydr. Polym., 258 (2021) 117644.
[33] Y. Liu, Is the free energy change of adsorption correctly calculated?, J. Chem. Eng. Data, 54 (2009) 1981–1985.
[34] M. Yılmazoğlu, N. Kanmaz, P. Demircivi, Constructing the synergistic effects of chitosan and ionic liquid on SPEEK polymer for efficient adsorption of crystal violet dye, Int. J. Biol. Macromol., 271 (2024) 132638.
[35] A. M. Omer, G. S. Elgarhy, G. M. El-Subruiti, E. M. Abd El-Monaem, A. S. Eltaweil, Construction of efficient Ni-FeLDH@MWCNT@Cellulose acetate floatable microbeads for Cr(VI) removal: Performance and mechanism, Carbohydr. Polym., 311 (2023)120771.
[36] Q. Wang, W.Zuo, Y. Tian, L. Kong, G. Cai, H. Zhang, L. Li, J. Zhang, An ultralight and flexible nanofibrillated cellulose/chitosan aerogel for efficient chromium removal: Adsorption-reduction process and mechanism, Chemosphere, 329(2023)138622.
[37] D. M. Guo, Q. Da An, Z. Y. Xiao, S. R. Zhai, and Z. Shi, Polyethylenimine-functionalized cellulose aerogel beads for efficient dynamic removal of chromium(VI) from aqueous solution, RSC Adv., 7 (2017) 54039–54052.
[38] X. Sun, L. Yang, Q. Li, J. Zhao, X.Li, X. Wang, H. Liu, Amino-functionalized magnetic cellulose nanocomposite as adsorbent for removal of Cr(VI): Synthesis and adsorption studies, Chem. Eng. J., 241(2014) 175–183.
[39] A. Karamipour, P. Khadiv Parsi, P. Zahedi, S. M. A. Moosavian, Using Fe3O4-coated nanofibers based on cellulose acetate/chitosan for adsorption of Cr(VI), Ni(II) and phenol from aqueous solutions, Int. J. Biol. Macromol.,154(2020)1132–1139.